

GA-A24335

**LAUNCHER PERFORMANCE IN
THE DIII-D ECH SYSTEM**

by

**K. KAJIWARA, C.B. BAXI, J. LOHR, Y.A. GORELOV,
M.T. GREEN, D. PONCE, and R.W. CALLIS**

JULY 2003

DISCLAIMER

This report was prepared as an account of work sponsored by an agency of the United States Government. Neither the United States Government nor any agency thereof, nor any of their employees, makes any warranty, express or implied, or assumes any legal liability or responsibility for the accuracy, completeness, or usefulness of any information, apparatus, product, or process disclosed, or represents that its use would not infringe privately owned rights. Reference herein to any specific commercial product, process, or service by trade name, trademark, manufacturer, or otherwise, does not necessarily constitute or imply its endorsement, recommendation, or favoring by the United States Government or any agency thereof. The views and opinions of authors expressed herein do not necessarily state or reflect those of the United States Government or any agency thereof.

LAUNCHER PERFORMANCE IN THE DIII-D ECH SYSTEM

by

K. KAJIWARA,* C.B. BAXI, J. LOHR, Y.A. GORELOV,
M.T. GREEN, D. PONCE, and R.W. CALLIS

This is a preprint of a paper to be presented at the 15th
Topical Conference on Radio Frequency Power in Plasmas,
Moran, Wyoming, May 19–21, 2003 and to be published in
the *Proceedings*.

*Oak Ridge Institute for Science Education, Oak Ridge, Tennessee.

Work supported by
the U.S. Department of Energy
under Contract Nos. DE-AC05-76OR00033, DE-AC03-99ER54463,
and DE-AC02-76CH03073

GENERAL ATOMICS PROJECT 30033
JULY 2003

Launcher Performance in the DIII-D ECH System

K. Kajiwara,^a C.B. Baxi, J. Lohr, Y.A. Gorelov, M.T. Green, D. Ponce,
and R.W. Callis

General Atomics, P.O. Box 85608, San Diego, California 92186-5608
^aORISE, Oak Ridge, Tennessee.

Abstract. The thermal performance of three different designs for the steerable mirrors on the ECH launchers installed in the DIII-D tokamak has been evaluated theoretically and experimentally. In each case the disruption forces must be minimized while providing a low loss reflecting surface. One design uses all Glidcop[®] material, but shaped so that the center is appreciably thicker than the edge. A second design is graphite with a molybdenum surface brazed to the graphite. The latest design is laminated copper/stainless steel construction with a thin copper reflecting surface. All three mirrors employ passive radiative cooling. The mirror temperatures are measured by resistance temperature devices (RTDs) which are attached at the back surfaces of the mirrors. The temperature increases are moderate for the laminated mirror, which has the best overall performance.

INTRODUCTION

Electron cyclotron (EC) waves can be used for plasma heating and current drive in tokamak devices. One important consideration is that the EC wave can be propagated in free space. Therefore, in a reactor the launcher can be located far from the plasma to reduce the neutron damage and employ miter bends which eliminate neutron leakage through the wave guide. Another advantage is that, because of the high electron cyclotron resonance frequency, steering of the rf beam using simple movable quasi-optical mirrors is possible. In free space propagation, the thermal performance of the mirrors becomes important, since the rf beam naturally assumes a Gaussian power profile with very high central power density. With the movable launcher mirrors located in the vacuum vessel, water cooling is difficult and results in serious problems in case of leaks. For non-CW rf operation with pulse lengths up to about ten seconds, enhancement of the radiation cooling from the back of the mirrors makes it possible to operate without active cooling. In DIII-D, five designs for passively cooled mirrors have been used. In this paper, we discuss the three most successful.

DIII-D ECH SYSTEM

The electron cyclotron heating (ECH) system consists of six 110 GHz gyrotrons and three launchers which include two wave guides each [1]. Three of the gyrotrons

were made by Communications and Power Industries (CPI) and the others were made by Gycom. The CPI gyrotrons have chemical vapor deposition (CVD) diamond output windows which supports 1 MW-10 s operation for Gaussian output rf beams [2]. The Gycom gyrotrons have boron nitride windows, which limit the pulse lengths for these tubes to 2 s with ~ 1 MW rf generation. The rf is transported by ~ 100 m of 31.75 mm diameter evacuated corrugated waveguide carrying the $HE_{1,1}$ mode. Each wave guide has a rf pair of grooved polarizers which can produce arbitrary elliptical polarization of the wave.

Each launcher has two sets of waveguides and mirrors. Each mirror set consists of a weakly focusing fixed mirror and a steerable flat mirror (Fig. 1). The steerable mirrors can direct the rf beams in the toroidal and poloidal directions. Each mirror has two RTDs at the back surface and each waveguide has one RTD to monitor temperature increases during the rf pulses. Each launcher has two Langmuir probes and a camera port for observation of possible arcing at the mirrors or waveguides.

MIRROR DESIGNS

Poloidal and toroidal steering is provided using movable mirrors of different designs to direct the rf beams. Eddy current induced forces arising during disruptions are particularly problematic for the actuator assemblies on the movable mirrors, which have limited ability to react the forces. The first attempt at designing launcher mirrors for DIII-D used graphite covered by evaporated molybdenum and thin copper coatings to create a low loss reflecting surface. The design was excellent thermally and had very low eddy current induced forces during disruptions. However, surface arcing on the mirrors during rf operation at relatively low energy levels generated gas and damaged the coatings.

An improved mirror design was made from Glidcop[®]. This mirror had a thin copper reflecting surface with a thicker center, or boss, to provide thermal inertia where the power density of the Gaussian beam was greatest. The back surface of this mirror was grooved and blackened to increase radiative cooling [Fig. 2(a)] [3]. This mirror was calculated to withstand a 10 s and 800 kW rf beam without excessive temperature increase or long term ratcheting from repeated pulses. However, the design suffers from relatively large disruptive eddy currents because of the volume of low resistivity Glidcop[®]. A robust actuator assembly was required to react forces with this mirror.

A modification of the graphite/molybdenum approach used a brazed molybdenum reflecting surface, which eliminated the arc damage, but had a relatively high resistivity and the highest surface temperature of the tested designs [Fig. 2(b)]. This modification did produce a mirror capable of 5 s 800 kW operation.

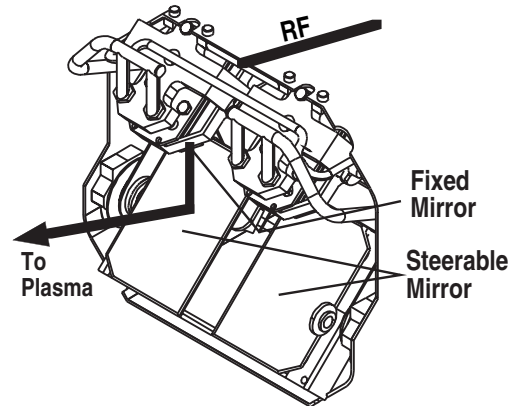


FIGURE 1. The launchers have weakly focusing fixed mirrors and flat steering mirrors with both poloidal and toroidal scan capability. Each launcher assembly accommodates the rf beams from two gyrotrons.

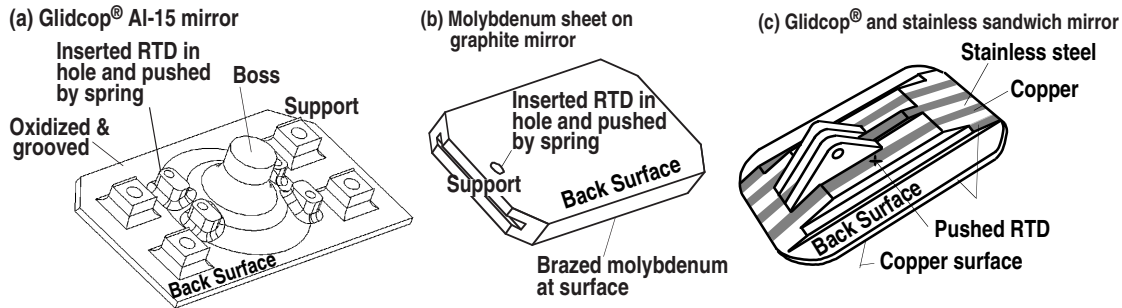


FIGURE 2. The thermal performance was studied for three different mirror designs: (a) Glidcop[®] mirror with a machined boss to increase the thermal mass with relatively low magnetic torques during disruptions, (b) graphite mirror with brazen molybdenum reflecting surface, (c) stainless steel and Glidcop[®] laminated structure with a thin copper reflecting surface supported by the sandwich.

The most recent mirror, with overall best performance, is called the “butcher block” mirror, which has a sandwich structure of Glidcop[®] and stainless steel [Fig. 2(c)]. The reflecting surface on this mirror is a thin copper layer supported by the sandwich. This structure can withstand modest disruption forces while providing a quality reflecting surface. The thermal performance allows rf pulses of 800 kW for 10 s. Heat is conducted from the reflecting surface by the Glidcop[®] and radiated to the surrounding structure. This design has the best overall performance of the three designs in the present study and meets the power, pulse length and duty cycle requirements for DIII-D experiments.

EXPERIMENTAL RESULTS

Measurements of the mirror temperatures during rf pulses into plasma discharges permit the three designs to be compared. The time dependencies of the RTD measurements are presented in Fig. 3(a) for the Glidcop[®], moly/graphite and butcher block mirrors. The rf power was 450–600 kW and the pulse width was 800 ms. Data for the Glidcop[®] mirror during the plasma discharge and for the first few seconds after are not available. The highest temperature was recorded for the moly/graphite mirror design because of high resistivity of the molybdenum surface. The butcher block mirror has two temperature peaks. The RTD is mounted on the copper part of the sandwich on the mirror back surface. The first peak results from conduction through the copper and the second peak is due to slower conduction through the stainless steel. The lowest peak temperature is observed for the Glidcop[®] mirror as expected, but the compromise here is that eddy current forces are higher for this mirror than for the others.

Disruptions result in additional mirror heating due to induced currents and increased plasma radiation impinging on the mirrors. Figure 3(b) shows the effect of a disruption on the moly/graphite launcher mirror. The curves are the time evolution of the RTD signals in the cases of normal plasma termination and disruptive termination of a 0.3 MA plasma. The plasma parameters for these two shots are similar, with central electron temperature of 2.7 keV and central density of $2.5 \times 10^{19} \text{m}^{-3}$. The

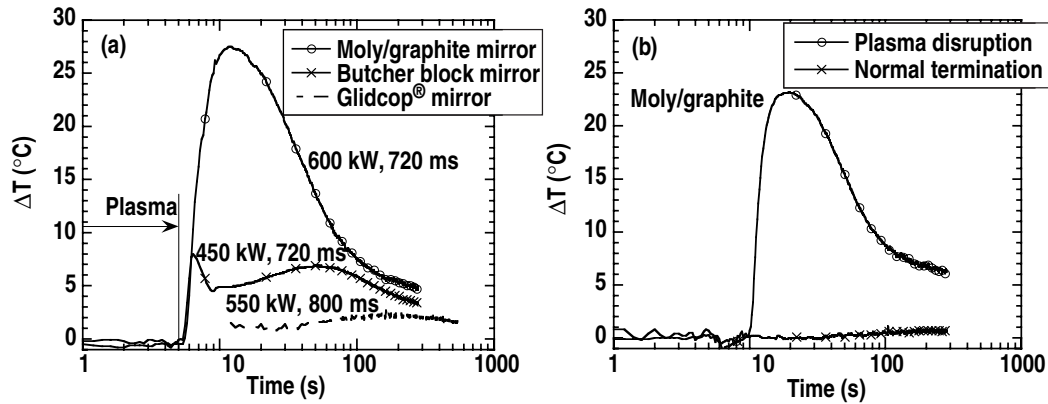


FIGURE 3. Time evolution of the temperature increase measured by the RTD for the different mirror designs: (a) Glidcop[®], moly/graphite and butcher block mirror with rf power of 450–600 kW and pulse width 720–800 ms (data for the Glidcop[®] mirror during plasma discharges and the first few seconds after a plasma discharge are not available); and (b) the moly/graphite mirror in the case of disruptive and normal plasma terminations.

temperature of the mirror is clearly increased by the disruption and the time dependence of the heating response is similar to the case of normal rf injection. The input power from the plasma to the mirror during the disruption is estimated at 20 kJ by comparing with calculations for rf injection.

The peak temperature is a function of the pulse length, as shown in Fig. 4. The peak temperature of the moly/graphite mirror is about five times higher than the butcher block. The butcher block mirror temperature is only slightly higher than the Glidcop[®] mirror, showing that the butcher block construction has good thermal performance in spite of the low eddy current design.

DISCUSSION

The solid lines in Fig. 4 show the peak temperature of the Glidcop[®] mirror calculated by finite element code COSMOS [4] at the RTD compared with measurements. The theoretical prediction is higher than the experimental result, by up to a factor of three. The discrepancy is understood to arise from poor thermal contact between the mirror and the RTD. In the vacuum situation, the RTD is mechanically pushed against the mirror, but without any heat conducting filler to improve the thermal contact. The thermal impedance for this installation is estimated by a simple experimental calibration. By holding an ice cube against the mirror surface with a thin plastic barrier sheet for 60 s, a known temperature reservoir can be applied to the mirror. The time evolution for this situation can be calculated by COSMOS as a function of the heat transfer between the ice cube

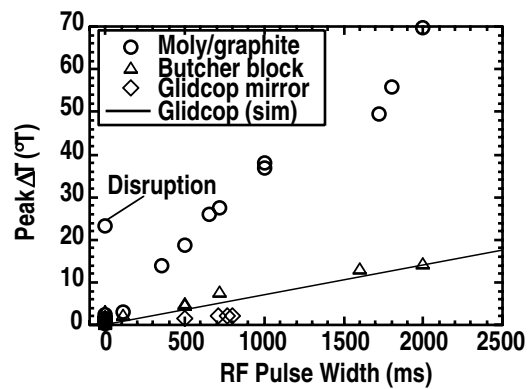


FIGURE 4. The peak temperature as a function of the rf pulse length. The solid line shows the simulation result for the Glidcop[®] mirror.

and mirror. The heat transfer coefficient between the ice and mirror is estimated by using additional temporary RTDs attached to the mirror using thermal grease to produce a good contact. These RTDs are attached at the center of mirror surface and the bottom near the position of the ice cube. Figure 5 shows the results. The time evolutions of measurements by the additional RTDs are well explained by the code, assuming a heat transfer coefficient of $1350 \text{ W/m}^2\text{K}$. By comparing the heat transfer coefficient inferred from the plasma measurements with this experimentally derived value, a thermal resistance of $2 \times 10^{-4} \text{ m}^2\text{K/W}$ for the case without grease is determined. Figure 6 shows the result of recalculation of the original heating measurements assuming this thermal resistance of $2 \times 10^{-4} \text{ m}^2\text{K/W}$ with good agreement between the COSMOS model and the measurements.

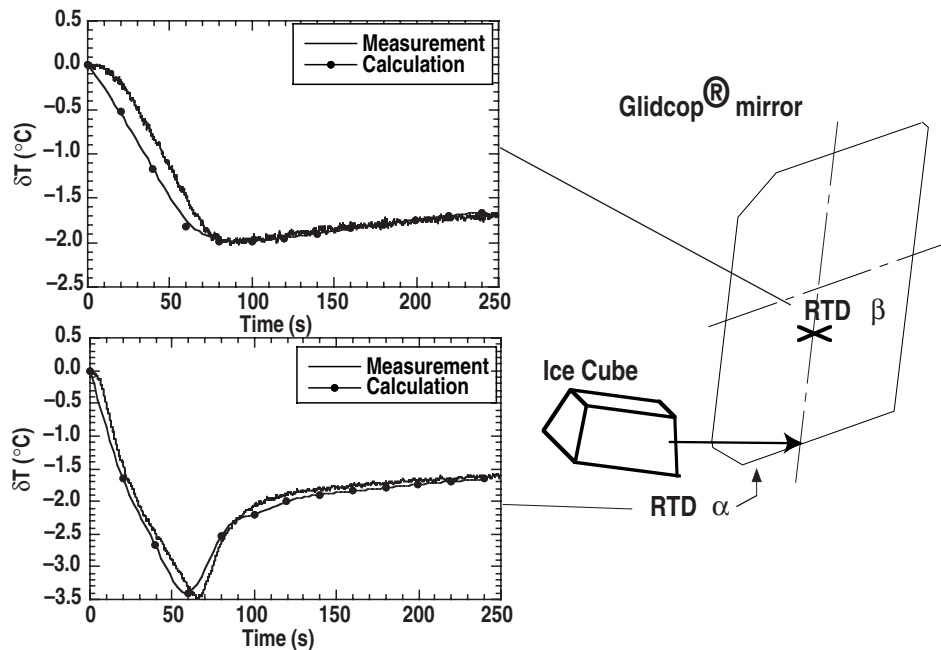


FIGURE 5. Experimental arrangement for the ice cube calibration in which the ice cube was held on the mirror surface through thin plastic for 60 s. The calculation assumes a heat transfer coefficient of $1350 \text{ W/m}^2\text{K}$ between the ice cube and mirror surface.

CONCLUSION

The temperature increases of three mirrors, a Glidcop® mirror, a mirror which was made from graphite with a brazed molybdenum surface, and a mirror which was made from a laminate of copper and stainless steel, are observed during rf pulses using RTDs which are attached at the back surfaces of the mirrors. The highest temperature increase was observed for the moly/graphite mirror and the lowest temperature was for the Glidcop® mirror, which has the best thermal performance. The temperature increase of the laminated mirror was moderately higher than the Glidcop® mirror, but lower than the molybdenum/graphite mirror. Because of the low eddy currents for the laminate design and the acceptable thermal performance, the design has been accepted for the DIII-D launcher systems.

ACKNOWLEDGMENT

Work supported by the U.S. Department of Energy under Contracts DE-AC03-99ER54463, DE-AC02-76CH03073, and DE-AC05-76OR00033. The author (K.K.) acknowledges R.A. Ellis at PPPL for providing the launchers.

REFERENCES

- [1] Lohr, J., et al., Proc. of 12th Joint Workshop on Electron Cyclotron Emission and Electron Cyclotron Resonance Heating (2002).
- [2] Gorelov, Y.A., et al., Proc. of 27th Int. Conf. on Infrared and Millimeter waves (2002).
- [3] Baxi, C.B., et al., Proc. of 19th IEEE/NPSS Symp. on Fusion Engineering (2002).
- [4] COSMOS, A Finite Element Analysis Code, Structural Research, Santa Monica, California, USA.

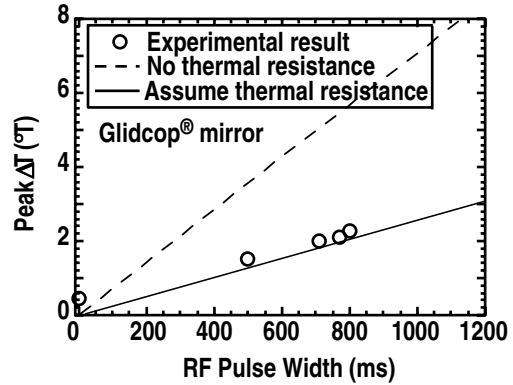


FIGURE 6. Peak temperature as a function of rf pulse width for the Glidcop[®] mirror. The dashed line is the previous calculation that is the same data in Fig. 4 solid line but with a recalculation made assuming the thermal resistance of $2 \times 10^{-4} \text{ m}^2\text{K/W}$ as determined in the ice cube experiments.